

Table of Contents

I

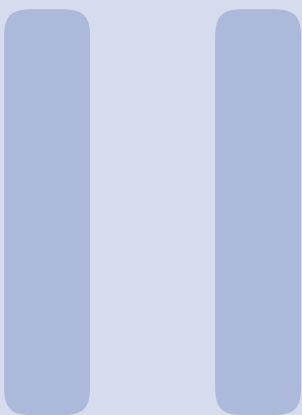
Theory and Experiment

II

Simulation, Processing and Analysis

1	The SPACE Analysis	7
1.1	Filter selection	7
1.1.1	VEF	7
1.1.2	LowUp	7
1.1.3	Online Muon L2	9
1.1.4	DeepCore	9
1.1.5	Burnsample checks	9
1.2	Level 3	9
1.2.1	Zenith angle cut	10
1.2.2	RlogL cut	10
1.2.3	NPE cut	11
1.2.4	Starting rlogL cut	11
1.2.5	Stopping rlogL cut	11
1.3	Level 4	11
1.3.1	Cleaning and quality cuts	12
1.3.2	Variable construction	13
1.4	Level 5	13
1.4.1	MRMR	13
1.4.2	BDT	13
1.5	Pull validation	14
1.6	Systematic Uncertainties	14
1.7	Results	14
2	Summary and Discussion	17

Appendices	21
A Gauge symmetries	23
B Planck's law	25
B.1 Electromagnetic waves in a cubical cavity	25
B.1.1 Classical approach	26
B.1.2 Quantum approach	26
C Statistics	27
D Distributions	29
D.1 Spherical random numbers	29
D.2 Power law distributions	30
D.3 Angular distributions	31
D.4 Weighting	32
E AdaBoost: simple example	35
3 Some useful things for LaTeX	37
3.1 Definitions	37
3.2 Remarks	37
3.3 Corollaries	37
3.4 Propositions	37
3.4.1 Several equations	38
3.4.2 Single Line	38
3.5 Examples	38
3.5.1 Equation and Text	38
3.5.2 Paragraph of Text	38
3.6 Exercises	38
3.7 Problems	38
3.8 Vocabulary	38
Bibliography	39
Index	41



Simulation, Processing and Analysis

1	The SPACE Analysis	7
1.1	Filter selection	
1.2	Level 3	
1.3	Level 4	
1.4	Level 5	
1.5	Pull validation	
1.6	Systematic Uncertainties	
1.7	Results	
2	Summary and Discussion	17

1. The SPACE Analysis

After introducing the detector workings, reconstruction and analysis techniques, background contributions and the signature of the signal, this chapter gives an overview of analysis. Starting from data processed with basic reconstructions and requirements a workflow was set up to try to discriminate events that are most likely of known physical interactions from the rare events that are sought for in this analysis. These events would originate from the theoretical particles with an anomalous charge (see Chapter ??). The analysis was adopted the "SPACE" analysis, which stands for a "Search for Particle with Anomalous ChargE".

1.1 Filter selection

As explained in Section ??, the data is processed through multiple filters. Since this analysis is the first of its kind in the collaboration, no processed dataset from other analyses was used. Filters had to be selected for proper comparison of data and Monte Carlo and I have chosen to optimize the signal to background ratio to select which filters should be included. An illustration is given in Fig. 1.1. This filter selection will be referred to as *Level2b*, as a simple addition to filter processing in Level2 (see Section ??).

1.1.1 VEF

The Vertical Event Filter (VEF) is designed to be used for oscillation and Earth WIMP analyses and makes use of the string trigger (see Section ??). An SMT that travel alongside a string, or closeby, can trigger optical modules while the total light yield of an event is low, making this filter an ideal addition to the filters that are selected. In addition, the filter removes HLC hits in the top 5 DOM layers to reduce the muonic component from air shower events. Other selection cuts, try to optimize the search efficiency for WIMP events in particular. For example, the LF zenith angle should be higher than 68.7° . More information can be found in Ref. [1].

1.1.2 LowUp

The LowUp filter is again mainly designed for WIMP searches, but also atmospheric neutrino analysis and is mainly designed to capture up-going muons with an energy below 1 TeV. The majority of the events that are selected by this filter make use of the in-ice Volume Trigger (see Table ??), but also the in-ice SMT8, in-ice String and SMT3-DeepCore triggers are run over for completeness. The selection cuts are loose selections required to look for up-going track-like particles. For example, the zenith angle of the reconstructed particle should have an angle of 80°

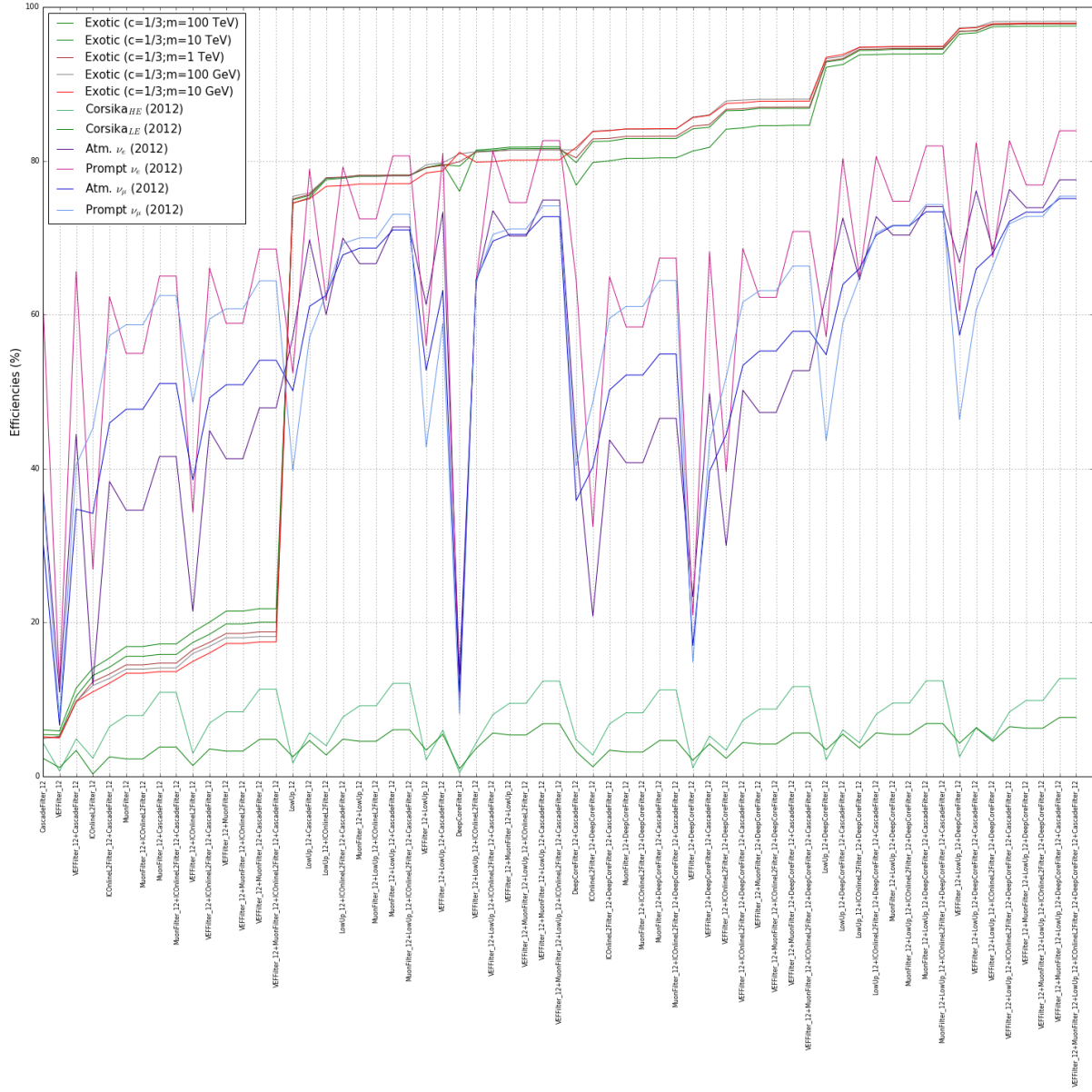


Figure 1.1: Illustration of the efficiencies of several filters and their possible combinations. The x-axis was determined by starting with filter selections that had a low efficiency in signal selection and range in function of performance. Five signal points for a fixed charge and different mass show similar results. Exotic SMPs with charges $1/2$ and $2/3$ show very similar results but are left out for a better visualization.

or higher and the difference between the maximal z-coordinate and minimal z-coordinate of hit DOMs should be less than or equal to 600 m. More information can be found in Ref. [2].

1.1.3 Online Muon L2

The Online Muon L2 filter is a subset of the Muon Filter (see Ref. ??) and tries to select the most interesting muon-like events while reducing the rate of the filter from around 30 Hz to 5 Hz, reducing the data with a factor of 6. Historically this subset was processed data from the Muon Filter, but after realizing that this could be done online and because many analyses made use of this selection, it was chosen to implement it as a separate filter. The filter tries to select both up-going and down-going muons, with different selection cuts depending on the zenith angle of the particle reconstruction. The four selection ranges are defined as:

- $180^\circ \geq \theta_{\text{MPE}} \geq 115^\circ$
- $115^\circ > \theta_{\text{MPE}} \geq 82^\circ$
- $82^\circ > \theta_{\text{MPE}} \geq 66^\circ$
- $66^\circ > \theta_{\text{MPE}} \geq 0^\circ$

where the particle reconstruction was done with MPE (Section ??), which was feasible if it only had to be done on the events passing the Muon Filter. The first two regions have an efficiency* higher than 99%. The down-going region require more stringent cuts to remove the less interesting muons from air showers. The variables used are the number of hit DOMs, likelihood parameters, number of PEs and so on. More information can be found in Ref. [3].

Verhoogt uw signaal niet zo veel omdat je enkel upgoing signaal gebruikte om dit te testen.

1.1.4 DeepCore

Additionally a DeepCore specialized filter was added to account for SMP tracks that partially traverse the more densely instrumented DC detector. Due to the low amount of light produced by these dim tracks, adding the DeepCore filter that is specialized for this part of the detector proved to be of significant importance.

The DeepCore filter was designed to look for very dim events coming from, e.g., dark matter, low-energy neutrino oscillations, and studies in observing atmospheric neutrinos below 100 GeV. The fiducial volume used for this filter consists of

- the bottom 22 DOMs on the IceCube strings 25, 26, 27, 34, 35, 36, 37, 44, 45, 46, 47 and 54;
- the bottom 50 DOMs on the DeepCore strings 79-86.

These strings are indicated in Fig. 1.2.

The filter uses the DeepCore SMT3 trigger and calculates the COG position. Two layers are used as a veto to remove events that probably originate from atmospheric muons. More information can be found in Ref. [4].

1.1.5 Burnsample checks

Before further processing, the burn sample (Section ??) is compared over the different years that are used in the analysis. This is shown in Figure 1.3. More information on the burn sample can be found in Section ??.

1.2 Level 3

The combined filter selection leads to a total rate of ~ 60 Hz, or ~ 1.9 billion events per year. The average event size at Level2 is around 15 kB, which would result into around 30 TB of data per year.

Therefore, five quality cuts are implemented with a goal that is threefold:

*Here defined as having a reconstruction within 3° of the MC truth.

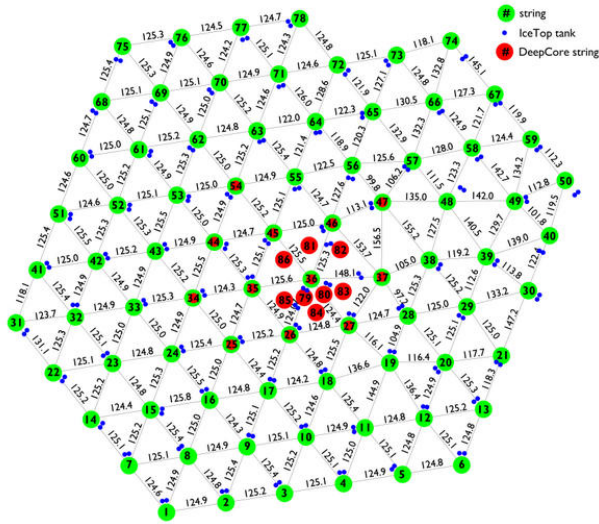


Figure 1.2: Aerial view of the IceCube strings (and IceTop tanks) where the DeepCore fiducial volume is defined by the DeepCore strings (red) and several surrounding in-ice IceCube strings (green and red).

1. reduce the total rate of the data,
2. improve the signal to background ratio, getting rid of uninteresting events,
3. improve the agreement between data and Monte Carlo.

These cuts are shown in Fig. 1.4.

1.2.1 Zenith angle cut

Even though there are no up-going muons from air showers expected, the vast majority of events that pass the filter selection remain from misreconstructed muons. Even though there is only a small chance of these events to have a large misreconstructed zenith angle. The expected flux of air showers is so much larger compared to the assumed signal flux to such an extent that it dominates with orders of magnitude. The majority still has a reconstructed zenith angle lower than 90° . Therefore the zenith angle cut was set at an angle of

$$\theta_{\text{zen}}(\text{MPE}) \geq 85^\circ. \quad (1.1)$$

1.2.2 RlogL cut

The reduced log-likelihood, rlogL of the track reconstruction fit is used as a goodness-of-fit variable. The term “reduced” is used because the logarithm of the likelihood is normalized by the number of degrees of freedom (NDOF) in the track fit

$$\text{rlogL} = \frac{\log \mathcal{L}}{\text{NDOF}} = \frac{\log \mathcal{L}}{\text{NCh} - \text{NPara}}, \quad (1.2)$$

where NCh is the number of channels/DOMs and NPara the number of fitted parameters (3 for the position and 2 for the track). For Gaussian probability distributions this expression corresponds to the reduced chi-square. Lower values indicate better reconstructions, therefore the rlogL cut was set at a value of

$$\text{rlogL} < 15. \quad (1.3)$$

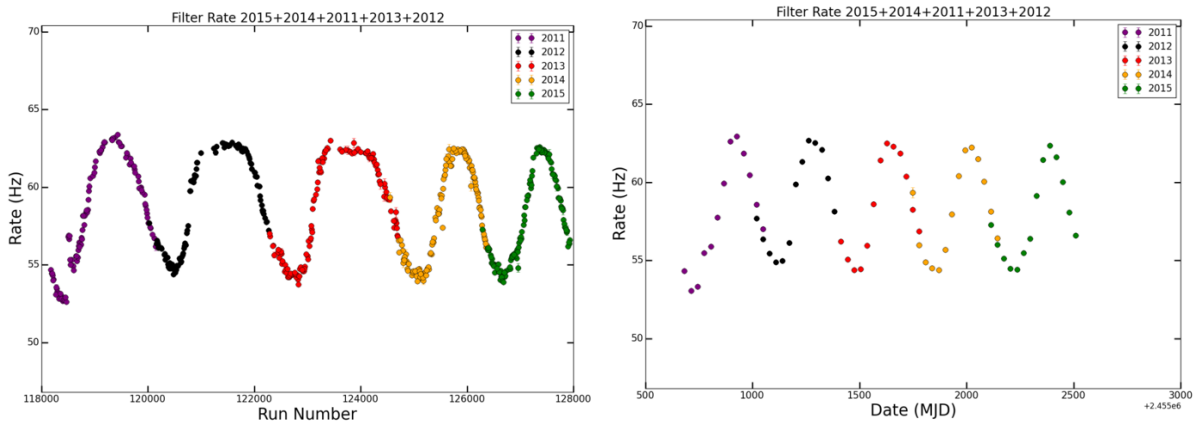


Figure 1.3: *Left:* Total rate of the combined filters in function of the run number. The sine wave pattern from seasonal variations in the atmosphere (see Section ??) is clearly visible and consistent throughout the years. The x-axis is more spread out in the first years as there were more test runs. The shift in data rate in early 2011 runs is due to the DOM software change that was introduced in the Summer of 2011 [5]. This phenomenon is well understood and since the changes are minimal it was chosen to keep these runs. *Right:* Total filter rate averaged per month. There is an overlap for each year because a new season doesn't necessarily start in the beginning of a month.

1.2.3 NPE cut

The number of photoelectrons seen in the detector has a clear correlation to the number of photons that were emitted from the track. From Eq. ?? it is clear that particles with a charge < 1 will produce less light. Therefore a cut on the total number of photoelectrons was set at a value of

$$\text{NPE} < 50. \quad (1.4)$$

1.2.4 Starting rlogL cut

The relative probability for tracks to be starting and/or stopping can be computed with FiniteReco (see Section ??). Because most low-energetic muons would be starting and/or stopping in the detector, these likelihoods prove to be a powerful tool in removing these events *. The llh is always compared to the llh of throughgoing tracks, hence the “relative probability”. It was chosen to place the starting rlogL at a value of

$$\text{rlogL} = \text{rlogL}(\text{starting}) - \text{rlogL}(\text{throughgoing}) > 0. \quad (1.5)$$

1.2.5 Stopping rlogL cut

Analogous to the previous cut, it was chosen to place the stopping rlogL at a value of

$$\text{rlogL} = \text{rlogL}(\text{stopping}) - \text{rlogL}(\text{throughgoing}) > 10. \quad (1.6)$$

1.3 Level 4

As can be seen in Fig. 1.4, most of the background still originates from air showers (referred to as CORSIKA). Due to the Level 3 quality cuts, the total rate was reduced from around ~ 60 Hz to ~ 2 Hz, low enough for more elaborate variables to be computed and more elaborate cleaning. In Level 4 I have implemented the IceHive splitting and cleaning tools (see Section ??) and rerun the particle reconstructions on these “new” events. Additional quality cuts were added to this

*High energetic muons will have a higher chance of being throughgoing, but would produce much more light than the dim tracks that are expected for the SMPs.

Table 1.1: Overview of quality cuts in Level 4.

Variable	Definition	Cut	Motivation
nCh	Number of hit DOMs	≥ 5	Allows for better reconstructions
nStr	Number of hit strings	≥ 2	Allows for better reconstructions
nStr_in	The number of hit inner strings. An inner string is not located at the edge of the detector	≥ 1	Reduce leak-in events
Fitstatus MPE	Status of MPE reconstruction	Status == 'OK'	Remove bad reconstructions
θ_{HC} (MPE)	Zenith angle cut on HiveCleaned pulses	$\geq 85^\circ$	Similar to cut explained in ???: focus on up-going tracks
Innerstring domination	See text inline	== True	See text inline

level to ensure higher quality events. An overview is given in Table 1.1. Finally, new variables were constructed to use in Level 5.

1.3.1 Cleaning and quality cuts

IceHive provides for a thorough cleaning method, sometimes resulting into events with a very low amount of hit DOMs. However, a minimal amount of hits is required to have reasonable and trustworthy particle reconstructions. Similarly, more than one string should have a hit to allow for better reconstructions due to the sparse distribution of the strings in the detector. Because light is able to reach the edge of the detector, even if the closest approach of the particle is tens or hundreds of meters away for very bright events, it would be near impossible to distinguish bright events far from the detector to dim tracks passing close by. Therefore, it was required that at least one string not on the edge of the detector should have hit DOMs to reduce these *leak-in events*. The zenith angle cut is re-introduced on the new event that should have better reconstructions due to cleaning and finally there is a requirement for “innerstring domination”.

Innerstring domination

There persist classes of events at the boundary of the detector, which can be a problem for an upgoing track analysis. This includes event classes as:

- (Leak in) Events which are heading towards the instrumented volume, but stop right before they reach it or pass next to, but not too far from, the detector. These leak light to the detector boundaries.
- (Boundary) Events that penetrate the detector very shallow on the boundary lines and possibly have a cascade at the endpoint. The events have rather cascade like characteristics.
- (Corner-clippers) Events that are throughgoing on the corners of the detector that have a COG at a corner of the detector.
- (Leak out) Events originating from a neutrino passing through almost the entire length of the detector and only have an interaction vertex right before leaving the detector. Depending on position and angle, the reverse direction of reconstruction can be of similar probability and thus a nuisance.

All these event classes are not well reconstructable or have a high uncertainty in the reconstruction. It is more feasible to remove these class of events to maintain a sample of well reconstructable events. This is done here by the requirement of innerstring domination.

DOMs are defined as outer DOMs if they are one of the following:

- part of a string on edge of the detector,
- on the bottom of strings 1-78,
- on the top of strings 1-78.

The innerstring domination is set to `True` when

$$\frac{\#\text{outer DOMs}}{\#\text{inner DOMs}} < 0.5. \quad (1.7)$$

Table 1.2: List of Commonvariables used in this analysis.

[†] Whenever one of the track characteristics variables is shown/mentioned, the suffix (e.g. _50) refers to the track cylinder that was used around the track.

Category	Variable	Description
Track Characteristics [†]	AvgDistToDom	The average distance of the DOMs to the reconstructed track, weighted by the total charge of each DOM.
	EmptyHits	The maximal track length along the reconstructed track that got no hits within a cylinder around the track.
	TrackSeparation	Distance how far the COG positions of the first and the last quartile of the hits are separated from each other.
	TrackDistribution	The track hits distribution smoothness value [-1;1] shows how smooth the hits of the given pulse series within the specified track cylinder radius are distributed along the track.
Hit Statistics	ZTravel	Z value of first quartile (in time) of the hit DOMs is calculated. ZTravel is the average difference of the z value of all hit DOMs with the first quartile z value.
	ZMax	The maximum z of all hit DOMs.
Time Characteristics	ZPattern	All first pulses per DOM are ordered in time. If a DOM position of a pulse is higher than the previous ZPattern is increased with +1. If the second pulse is located lower in the detector ZPattern decreases with -1. In general this variable gives a tendency of the direction of a track.

1.3.2 Variable construction

To distinguish signal from background events, variables that show a clear distribution difference prove to have the most discriminative power. In this part of the analysis, multiple new variables are introduced with this goal. Some variables used in Level 5 are already explained in the text and need no further introduction. A summary is given in Table ??.

1.3.2.1 Commonvariables

Variables that were often used in analyses often had subtle differences between them, making them prone to be a cause of errors. Multiple variable were therefore combined into one project, called “Commonvariables”. The variables used here can be subdivided into three categories: track characteristics, hit statistics and time characteristics and are summarized in Table 1.2.

Because DC and IC DOMs have different quantum efficiencies (see Section ??), the pulses from DC and IC DOMs should not be mixed for an unambiguous definition. Therefore either only DC or IC pulses are used to compute these variables depending on if an event is *IC dominated* or *DC dominated*, where the former is set at $\frac{\#DOMs_{IC}}{\#DOMs_{DC}} \geq 0.5$ and the latter otherwise.

1.3.2.2 Millipede variables

The **Millipede** toolkit was introduced in Section ??, where it was explained how the energy deposition could be estimated from the light seen by the individual DOMs. Constructing multiple variables from this toolkit was the master thesis subject of Stef Verpoest and can be found in Ref. [6] for an elaborate explanation.

1.3.2.3 New variables

1.4 Level 5

1.4.1 MRMR

1.4.2 BDT

<https://arxiv.org/pdf/physics/0312102v1.pdf>

<https://arxiv.org/pdf/1310.1284.pdf>

Table 1.3: My caption

Class	Variable	MRMR score	Importance	MRMR score	Variable
Commonvariables	ZMax	2	0.109	1	NewLength_150
	ZTravel	3	0.106	2	ZMax
	AvgDistToDom_150	9	0.048	3	ZTravel
	TrackSeparation_150	10	0.043	4	RunsAboveMean
	TrackDistribution_50	12	0.035	5	Mean_dEdX
	TrackSeparation_50	13	0.034	6	NewLength_all_z
	EmptyHits_100	16	0.027	7	LineFit_Velocity
	ZPattern	17	0.016	8	σ_{para}
Millipede	RunsAboveMean	4	0.105	9	AvgDistToDom_150
	Mean_dEdX	5	0.074	10	TrackSeparation_150
	TrackLength_60	11	0.039	11	TrackLength_60
New variables	NewLength_150	1	0.132	12	TrackDistribution_50
	NewLength_all_z	6	0.059	13	TrackSeparation_50
	SpeedRatio	14	0.033	14	SpeedRatio
Other variables	LineFit_Velocity	7	0.055	15	$\cos(\theta)_{\text{SPE}}$
	σ_{para}	8	0.051	16	EmptyHits_100
	$\cos(\theta)_{\text{SPE}}$	15	0.033	17	ZPattern

Ook ergens een tabel maken met info over je data runs. Duidelijk maken wat de lifetime is bv en ook zeggen van wanneer to wanneer een bepaalde run liep (2011: mei 2011- mei 2012)

Klaus zijn paper? <https://arxiv.org/abs/1806.05696>

1.5 Pull validation

1.6 Systematic Uncertainties

1.7 Results

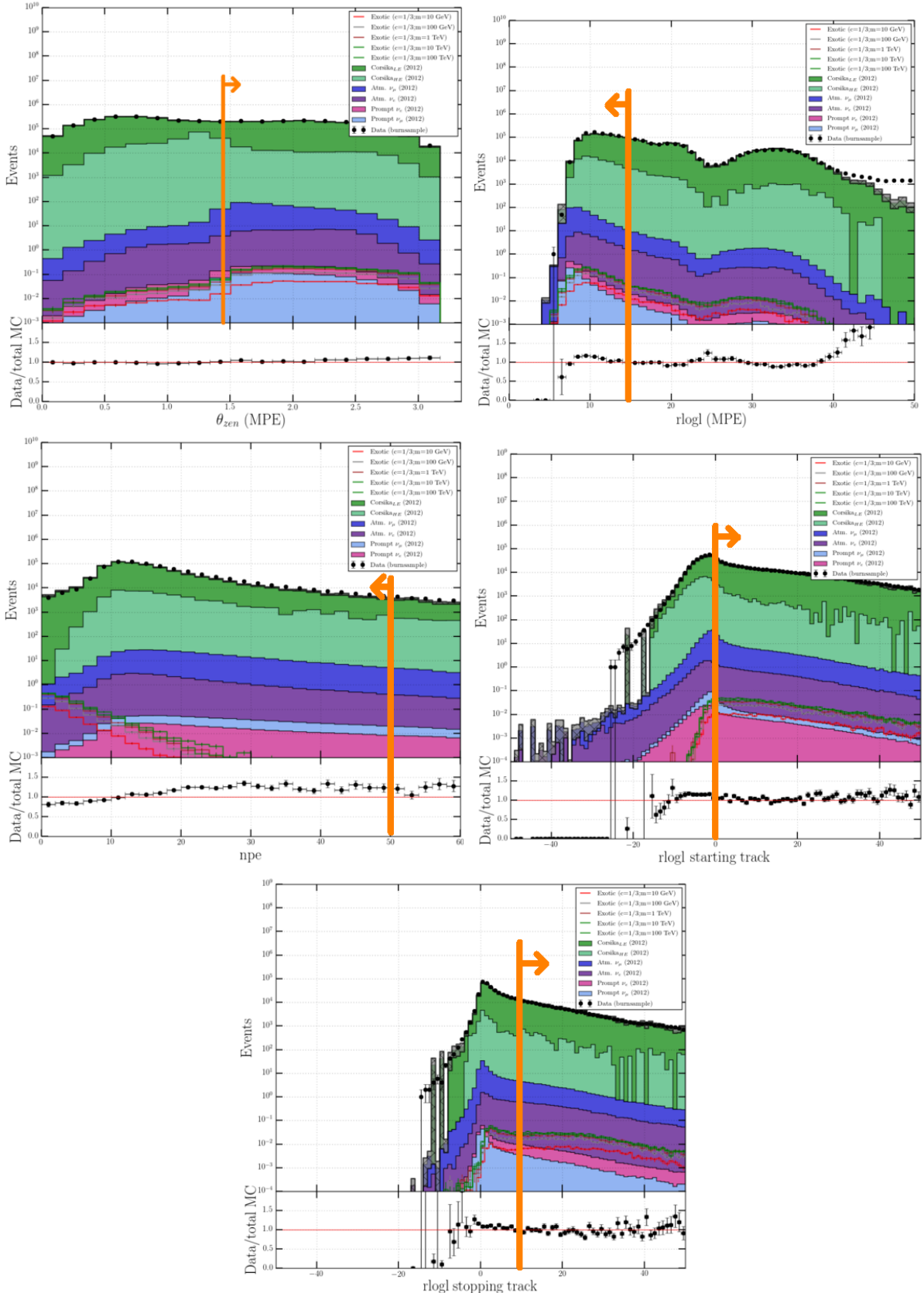


Figure 1.4: *First row, left:* Number of events in function of MPE reconstructed zenith angle normalized to the burn sample. The upwards trend to higher zenith angles is due to the filter selections that depend on the angle. *First row, right:* Number of events in function of $r\log L$ normalized to the burn sample. *Second row, left:* Number of events in function of number of photoelectrons (NPE) seen in the detector. *Second row, right:* Number of events in function of the starting likelihood. *Third row:* Number of events in function of the stopping likelihood. The cuts are illustrated with an orange line, the arrow points towards the events that are kept.

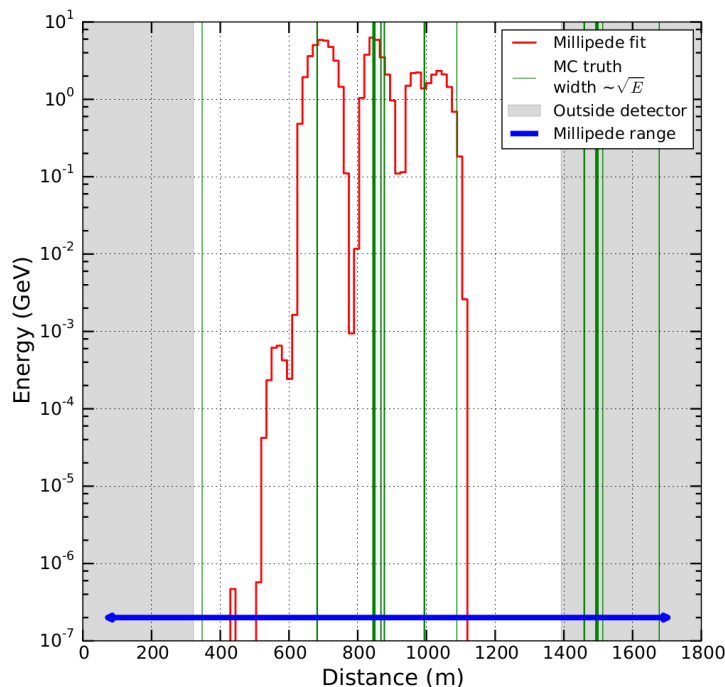


Figure 1.5: Output of a `Millipede` fit for an SMP with charge $\frac{1}{3}$ and mass 10 GeV. The x-axis shows the distance the particle traveled and starts after the first simulated energy loss event. The fit tries to estimate the energy of 15 m track segments. As a comparison, the true positions of energy deposits from the MC simulation are shown in green. Locations outside the detector are shaded in grey.



2. Summary and Discussion

Possible improvements: filter! Trigger! a speed cut... If multiple COGs, connection of both should be within time window.

Other machine learning techniques.

Energy estimators (although probably wrong)

Additions

Appendices 21

A **Gauge symmetries** 23

B **Planck's law** 25

B.1 Electromagnetic waves in a cubical cavity

C **Statistics** 27

D **Distributions** 29

D.1 Spherical random numbers

D.2 Power law distributions

D.3 Angular distributions

D.4 Weighting

E **AdaBoost: simple example** 35

3 **Some useful things for LaTeX** 37

3.1 Definitions

3.2 Remarks

3.3 Corollaries

3.4 Propositions

3.5 Examples

3.6 Exercises

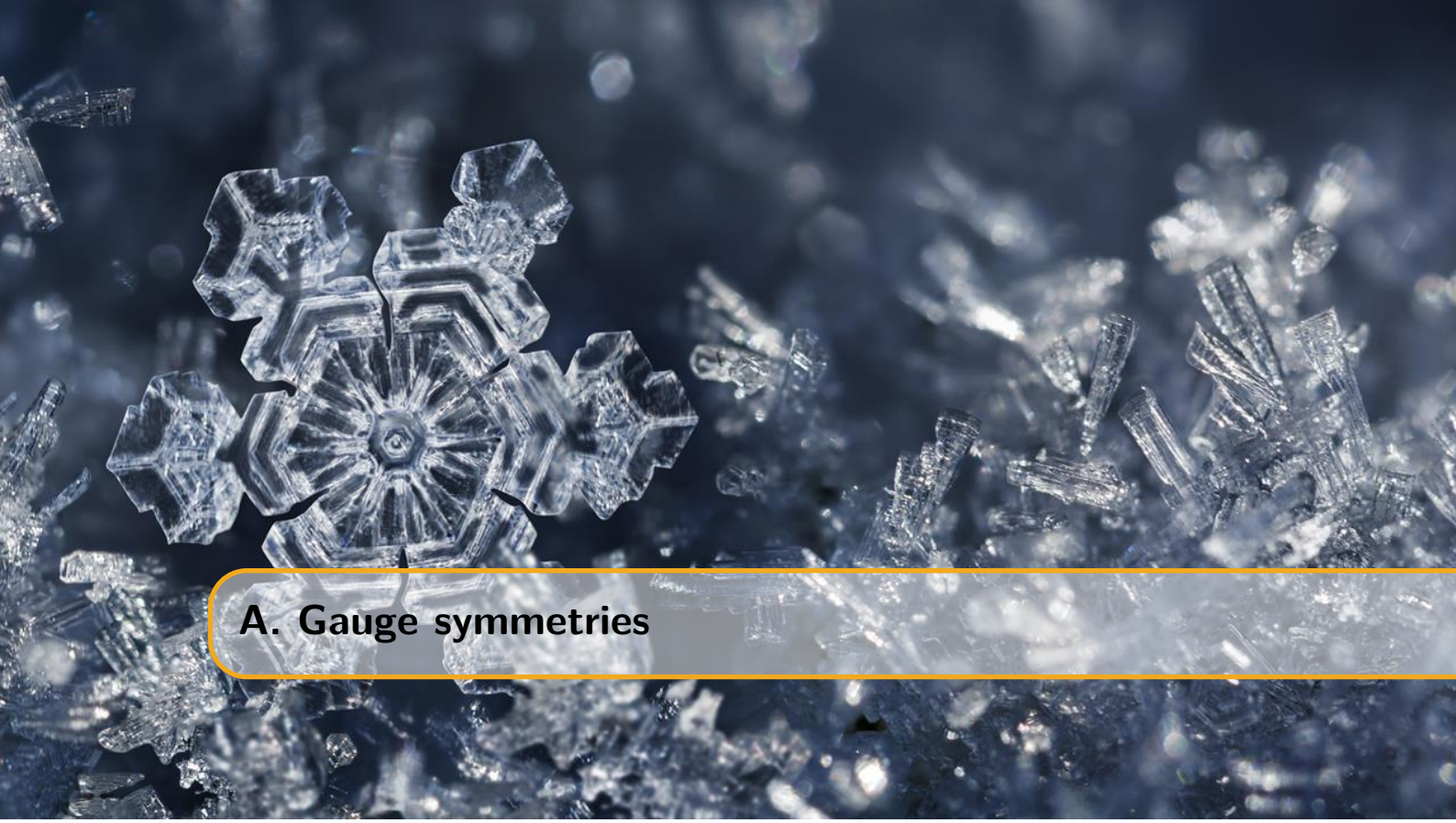
3.7 Problems

3.8 Vocabulary

Bibliography 39

Index 41

Appendices



A. Gauge symmetries

NOG NIET GEDAAN

The difference between global and local symmetries are not straightforward for everybody. In this appendix I try to give a better view of the matter.

Imagine that at each point in space and time there is a circle attached to it. If one shifts all circles of all points with a fixed angle the underlying physics hasn't changed. If we look at the whole in a different angle, nothing seems to be changed as everything holds the same relative orientation. This is a global symmetry. For local symmetries we instead shift each circle through a different angle, but an angle that changes smoothly from point to point and in a way that we can say how that angle is varying between different nearby regions. Then it will turn out that we can describe that rotation angle by means of a so-called gauge field, which just lets us transport the charged scalar field from one point in space time to another, taking account of how the rotation angle of the circle is changing. A gauge is a kind of coordinate system that is varying depending on the location with respect to some underlying space. In physics we are almost always concerned with space-time as the underlying space, and we are typically interested in theories that are invariant with respect to the choice of gauge or coordinate system.

Dan wat uitleg vanuit je QFT boek en de dingen hieronder: Je wilt je derivative anders doen werken in je theory onder een transformatie, maar daarvoor heb je een veld nodig. M.a.w.: dankzij een veld heb je lokale ijktransformatie mogelijk!

B. Planck's law

bron: <http://hyperphysics.phy-astr.gsu.edu/hbase/quantum/rayj.html>

B.1 Electromagnetic waves in a cubical cavity

Suppose we have EM waves in a cavity at equilibrium with its surroundings. These waves must satisfy the wave equation in three dimensions:

$$\frac{\partial^2 \Psi}{\partial x^2} + \frac{\partial^2 \Psi}{\partial y^2} + \frac{\partial^2 \Psi}{\partial z^2} = \frac{1}{c^2} \frac{\partial^2 \Psi}{\partial t^2}. \quad (\text{B.1})$$

The solution must give zero amplitude at the walls. A non-zero value would mean energy is dissipated through the walls which is in contradiction to our equilibrium assumption. A general solution takes the form of

$$\Psi(x, y, z, t) = \Psi_0 \sin k_1 x \sin k_2 y \sin k_3 z \sin k_4 t, \quad (\text{B.2})$$

which, after requiring $k_n L = n\pi$ with $n = 0, 1, 2, \dots$ and $k_4 \frac{\lambda}{2c} = \pi$, leads to

$$\Psi(x, y, z, t) = \Psi_0 \sin \left(\frac{n_1 \pi x}{L} \right) \sin \left(\frac{n_2 \pi y}{L} \right) \sin \left(\frac{n_3 \pi z}{L} \right) \sin \left(\frac{2\pi c t}{\lambda} \right). \quad (\text{B.3})$$

From the wave equation it is easy to find that

$$n^2 = n_1^2 + n_2^2 + n_3^2 = \frac{4L^2}{\lambda^2}, \quad (\text{B.4})$$

which span up a sphere in “n-space” with a volume of $\frac{1}{8} \frac{4}{3} \pi n^{3/2}$, where the first term originates from the positive nature of $n_{1,2,3}$. Because there are two possible polarizations of the waves one has to multiply with an additional factor 2. The number of modes per unit wavelength is equal to

$$\frac{dN}{d\lambda} \times \frac{1}{L^3} = \frac{d}{d\lambda} \left[\frac{8\pi L^3}{3\lambda^3} \right] \times \frac{1}{L^3} = - \left[\frac{8\pi}{\lambda^4} \right]. \quad (\text{B.5})$$

B.1.1 Classical approach

Following the principle of equipartition of energy, each standing wave mode will have an average energy kT with k the Boltzmann constant and T the temperature in Kelvin. The energy density is then:

$$\frac{du}{d\lambda} = -kT \frac{8\pi}{\lambda^4}. \quad (\text{B.6})$$

In function of frequency $\nu = \frac{c}{\lambda}$:

$$\frac{du}{d\nu} = -\frac{c}{\lambda^2} \frac{du}{d\lambda} = \frac{8\pi k T \nu^2}{c^3}, \quad (\text{B.7})$$

also known as the Rayleigh-Jeans law*. Problem: divergence

B.1.2 Quantum approach

The energy levels from a quantized harmonic oscillator are equal to

$$E_r = h\nu \left(r + \frac{1}{2} \right) = \frac{hc}{\lambda} \left(r + \frac{1}{2} \right) \quad \text{with } r = 0, 1, 2, \dots \quad (\text{B.8})$$

Implementing eq. B.4

$$E = \left(r + \frac{1}{2} \right) \frac{hc}{2L} \sqrt{n_1^2 + n_2^2 + n_3^2} \quad (\text{B.9})$$

According to statistical physics the average energy is now not equal to kT but follows a probability distribution

$$p(\nu, r) = \frac{e^{-r h \nu}}{\sum_{r=0}^{\infty} e^{-r h \nu}}, \quad (\text{B.10})$$

where we reference to the ground state of the oscillator: $E'_r = E_r - E_0$.

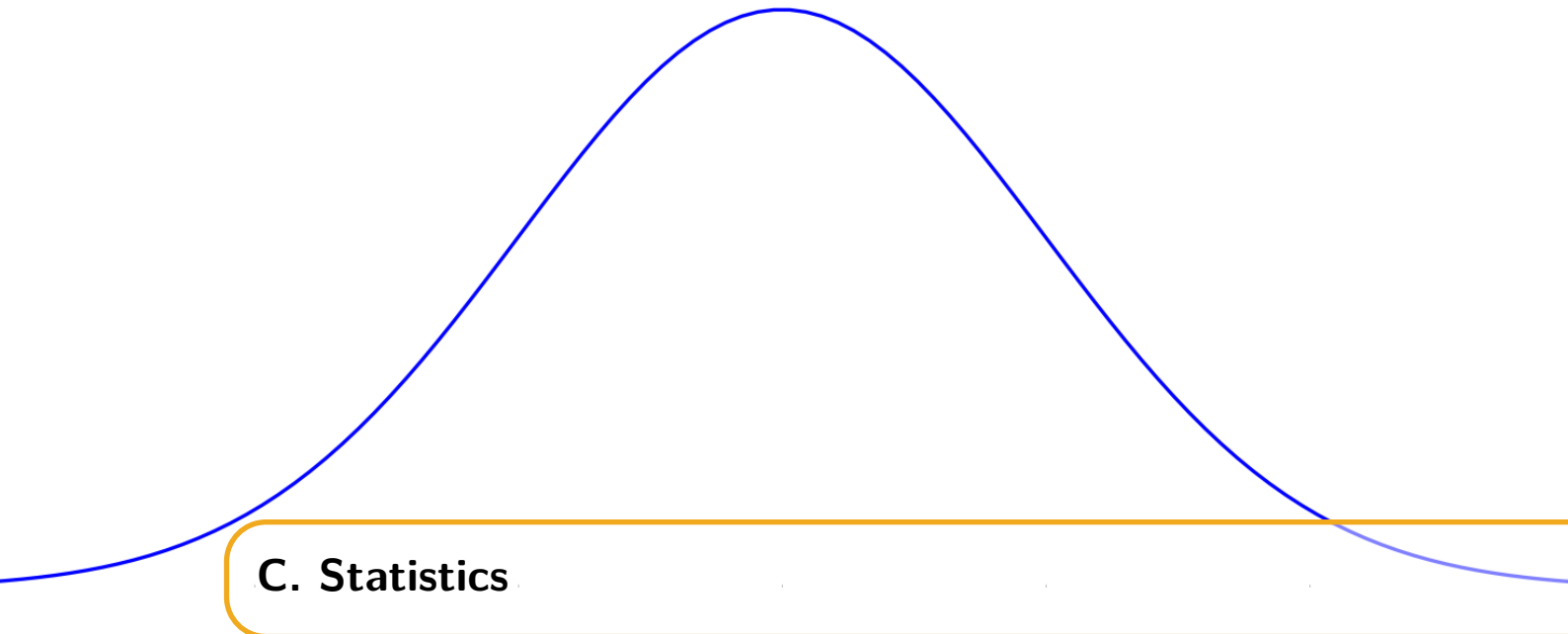
The average energy is now:

$$\begin{aligned} \langle E(\nu) \rangle &= \sum_{r=0}^{\infty} E(\nu, r) \cdot p(\nu, r) = \frac{\sum_{r=0}^{\infty} r h \nu e^{-r h \nu}}{\sum_{r=0}^{\infty} e^{-r h \nu}} \\ &= \frac{h \nu}{e^{h \nu / k T} - 1} \end{aligned} \quad (\text{B.11})$$

Substituting this for kT in eq. B.7 we find Planck's equation:

$$\frac{du}{d\nu} = \frac{8\pi h \nu^3}{c^3} \frac{h \nu}{e^{h \nu / k T} - 1} \quad (\text{B.12})$$

*This is often quoted per unit of steradian, which results in $\frac{2kT\nu^2}{c^3}$



C. Statistics

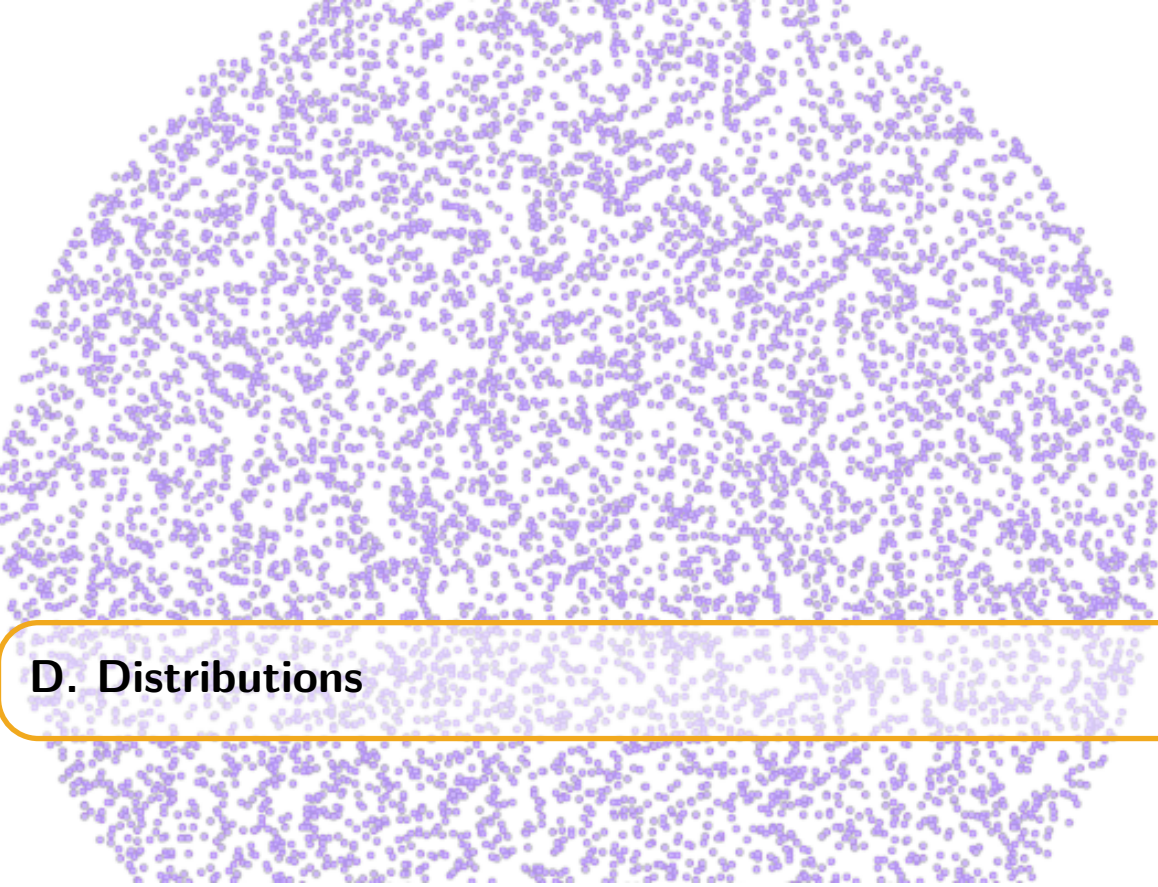
A word that is often mentioned in this work is “statistics”. It refers to the statistical error of a counting experiment, i.e. the Poissonian error. The Poisson distribution is a discrete probability of a certain number of n_{events} occurring in a fixed time interval. The Poisson probability function is given by

$$P(n) = \frac{\lambda^n e^{-\lambda}}{n!}, \quad (\text{C.1})$$

where λ is the expected number of events and also equal to the variance. An experiment that counted N events therefore has a statistical error of

$$\sigma = \sqrt{N} \quad (\text{C.2})$$

In other words: higher statistics denotes a lower statistical error.



D. Distributions

D.1 Spherical random numbers

Most random number generators provide uniform distributions between the range $[0, 1]$. Assume we want to make a uniform distribution along a sphere with angles ϕ and θ and radius r , in spherical coordinates. Random numbers between $[0, \pi]$, $[0, 2\pi]$ and $[0, R]$ (the ranges of the coordinates) would not give a uniform distribution as illustrated in Fig. D.1 (left).

The differential surface area, dA , is equal to $dA(d\phi, d\theta) = r^2 \sin(\phi) d\phi d\theta$. If we want the distribution $f(v)$ to be constant for a uniform distribution, then $f(v) = \frac{1}{4\pi}$ since $\int \int_S f(v) dA = 1$ and $\int \int_S dA = 4\pi$. We want the distribution in function of the angles, so

$$f(v)dA = \frac{1}{4\pi} dA = f(r)f(\phi, \theta)d\phi d\theta. \quad (\text{D.1})$$

Since we know the expression for dA , we find that

$$f(\phi, \theta) = \frac{1}{4\pi} \sin(\phi), \quad (\text{D.2})$$

and separating the angles:

$$f(\theta) = \int_0^\pi f(\phi, \theta) d\phi = \frac{1}{2\pi}, \quad (\text{D.3})$$

$$f(\phi) = \int_0^{2\pi} f(\phi, \theta) d\theta = \frac{\sin(\phi)}{2}, \quad (\text{D.4})$$

where it is clear that $f(\phi)$ scales with $\sin(\phi)$; there are more points needed at the equator (this makes sense, as the surface at the equator is much larger!).

The question is now how one can get a sample to follow the distribution of $f(\phi)$. For this, we use the *inverse transform sampling* method where one makes use of the cumulative distribution function, $F(\phi)$, which increases monotonically

$$F(\phi) = \int_0^\phi f(\phi') d\phi' = \frac{1}{2} (1 - \cos(\phi)). \quad (\text{D.5})$$

The method shows that if u is a random variable drawn from a uniform distribution, we have to find the inverse function of F ,

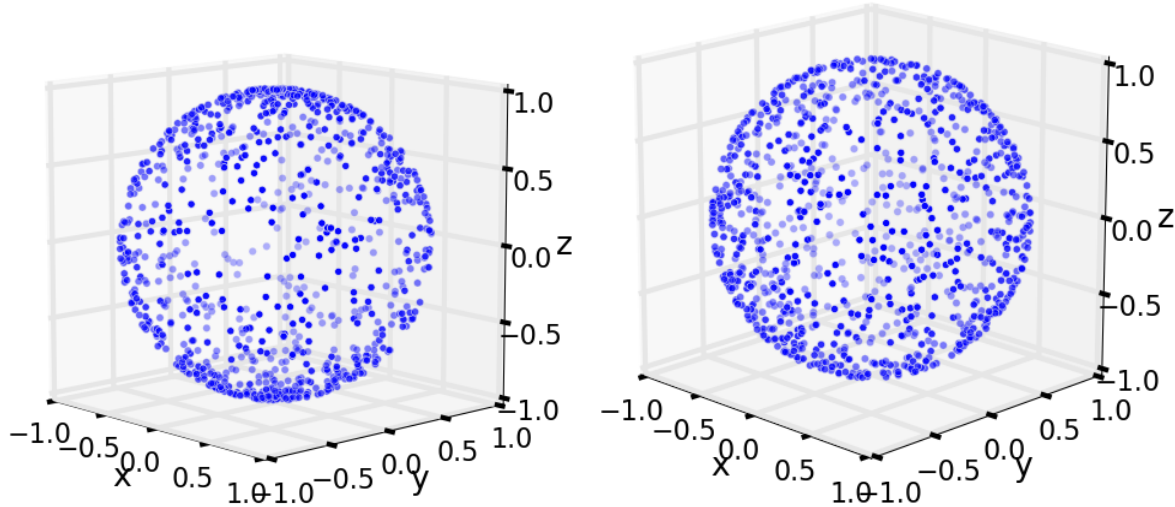


Figure D.1: *Left:* Illustration of a uniform sampling in angles ϕ and θ that doesn't give a uniform spherical distribution. *Right:* Illustration of a good spherical distribution.

$$F(F^{-1}(u)) = u \quad (\text{D.6})$$

$$\frac{1}{2} (1 - \cos(F^{-1}(u))) = u \quad (\text{D.7})$$

$$F^{-1}(u) = \arccos(1 - 2u). \quad (\text{D.8})$$

In other words: if u is a random variable drawn from a uniform distribution, then $\phi = \arccos(1 - 2u)$ follows a distribution necessary for a uniform spherical distribution. Similarly, $\theta = \frac{1}{2\pi}u$.

D.2 Power law distributions

Analogous to what was written in the previous section, one can produce a power law distribution from random numbers using the inverse transform sampling method:

$$\begin{aligned} f(E) &= A \cdot E^{-\gamma} \quad (\text{powerlaw}) \\ F(E) &= \int_{E_{min}}^E A \cdot E^{-\gamma} dE = u \quad (\text{inverse sampling, } u \text{ random number } [0,1]) \\ &= A \left[\frac{E^{-\gamma+1}}{-\gamma + 1} \right]_{E_{min}}^E \\ &= \frac{A}{-\gamma + 1} (E^{-\gamma+1} - E_{min}^{-\gamma+1}) \end{aligned} \quad (\text{D.9})$$

Because we know that $F(F^{-1}(u)) = u$, we can find an expression for $F^{-1}(u)$:

$$\begin{aligned} u &= \frac{A}{-\gamma + 1} \left((F^{-1}(u))^{-\gamma+1} - E_{min}^{-\gamma+1} \right) \\ &\Rightarrow \end{aligned} \quad (\text{D.10})$$

$$F^{-1}(u) = \left(\left(\frac{-\gamma + 1}{A} \cdot u \right) + E_{min}^{-\gamma+1} \right)^{1/(-\gamma+1)}$$

To find A , we use the property of a CDF:

$$F(E_{max}) = 1 \Rightarrow A = \frac{-\gamma + 1}{E_{max}^{-\gamma+1} - E_{min}^{-\gamma+1}}, \quad (\text{D.11})$$

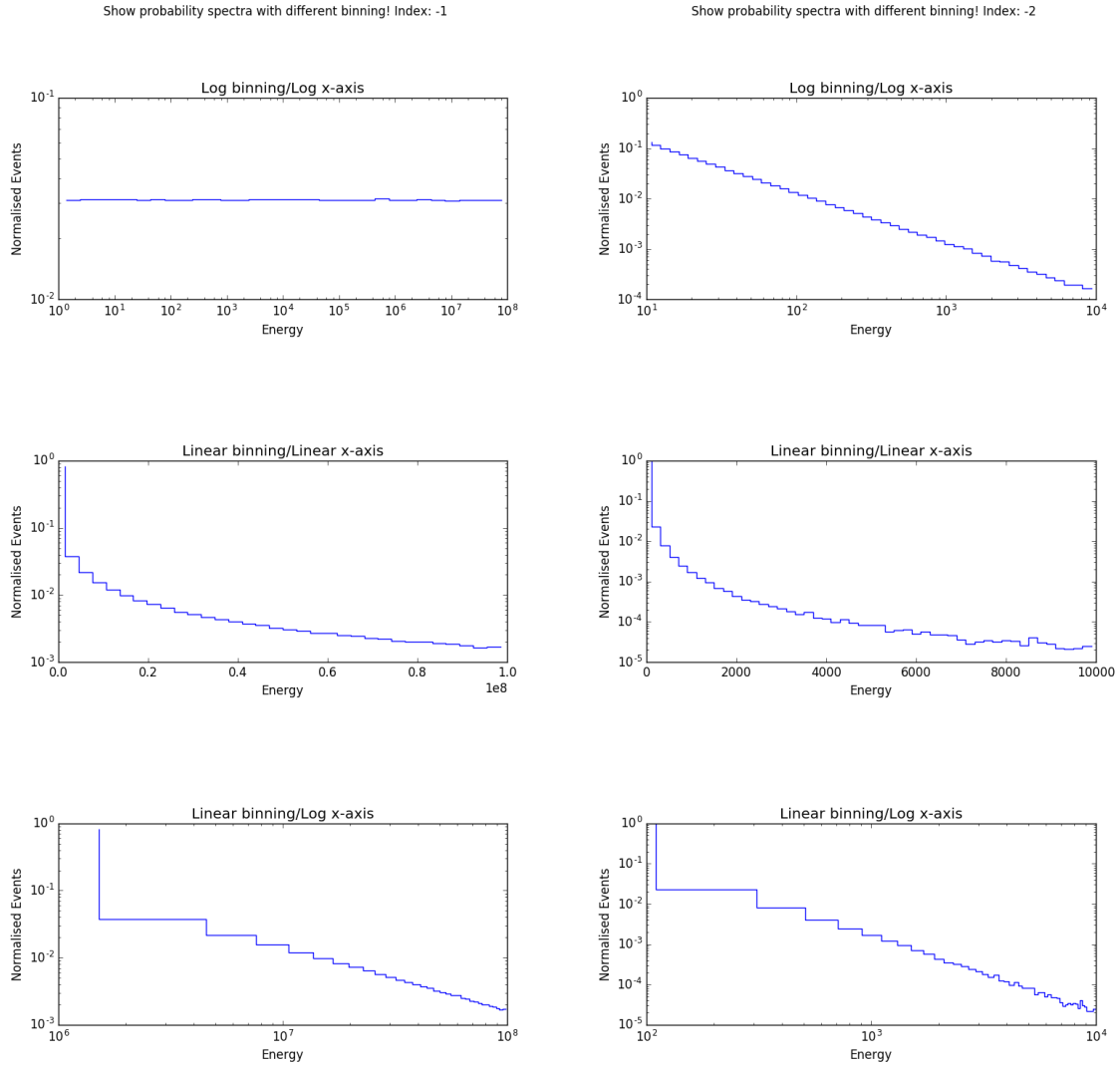


Figure D.2: *Left:* Histograms with different binnings showing the behavior of an energy spectrum with spectral index -1. *Right:* Histograms with different binnings showing the behavior of an energy spectrum with spectral index -2.

leading to

$$F^{-1}(u) = \left((1-u) \cdot E_{min}^{-\gamma+1} + u \cdot E_{max}^{-\gamma+1} \right)^{1/(-\gamma+1)}, \quad (\text{D.12})$$

which shows how one can draw a distribution in function of E following $f(E)$ with a uniform random number u .

For $\gamma = -1$, the computations are analogous and one can see that this will produce a uniform distribution in log space. This is shown in Fig. D.2.

$$\begin{aligned} E &= E_{min} \cdot 10^{u \cdot \log \frac{E_{max}}{E_{min}}} \\ &= 10^{u[\log E_{min}, \log E_{max}]} \end{aligned} \quad (\text{D.13})$$

In Fig. D.3 the signal reweighting is shown.

D.3 Angular distributions

As seen in Section D.1, the differential space angle $d\Omega$ is equal to

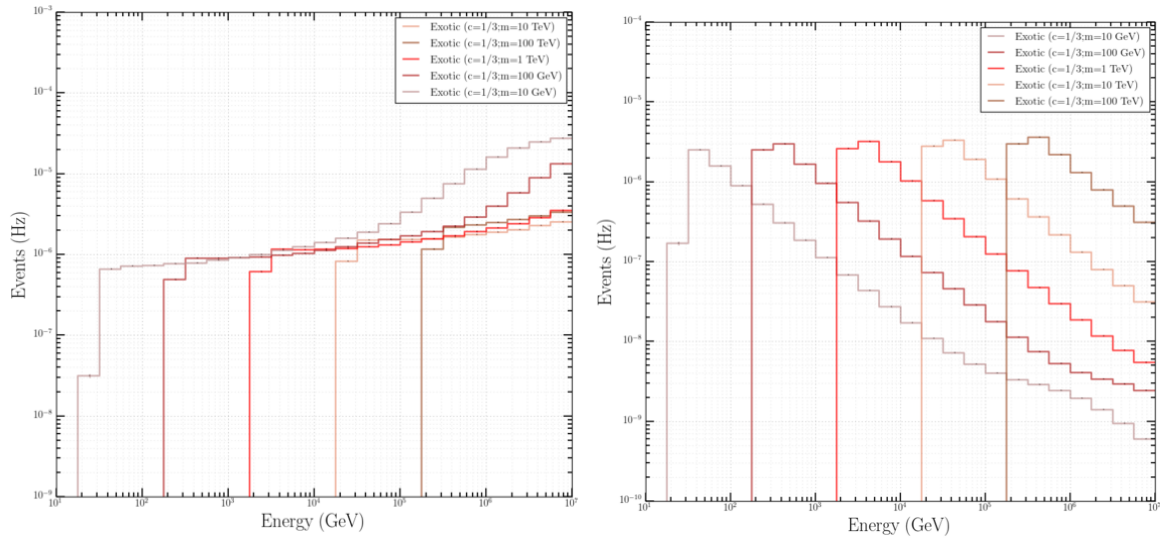


Figure D.3: *Left:* Spectrum of the signal before weighting following an E^{-1} spectrum. The rise in the rate in function of energy is due to the trigger efficiency that increases in function of energy. *Right:* Spectrum of the signal after reweighting to an energy spectrum of $E-2$.

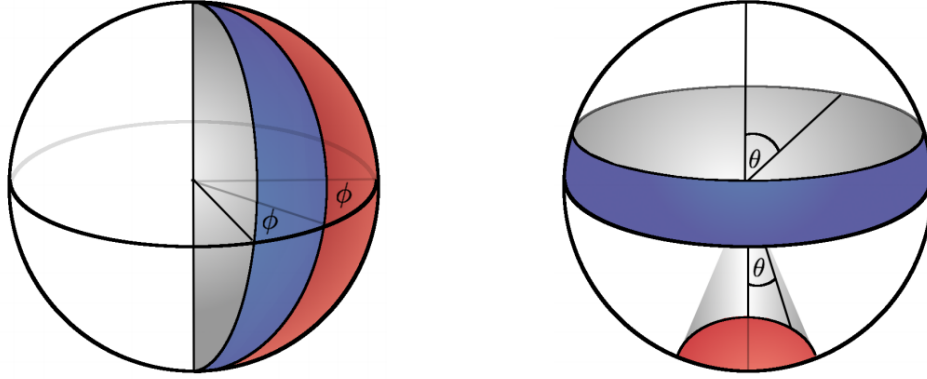


Figure D.4: Illustration of angle distributions in spherical coordinates. The blue and red surfaces are equal in size. The left figure clearly shows the surface to be proportional to the azimuth. The right figure shows how there is a non-trivial dependence on the zenith angle for equal partitions on the surface of a sphere.

$$d\Omega = \sin(\theta)d\theta d\phi. \quad (\text{D.14})$$

If one shows the distribution of ϕ and/or θ , then this is the same as showing partial integrations per bin. We find that

$$\Omega \propto \cos(\theta), \quad (\text{D.15})$$

or in other words: the space angle is proportional to the azimuth and the cosine of the zenith. An example is shown in Fig. D.4.

D.4 Weighting

A method that is often used in simulations is *weighting*. The simulated and expected differential flux of particles is often not the same, mainly due to two reasons:

- The flux has no uniform power law behavior. As can be seen in Fig. ??, there can be multiple “kinks” and changes in a spectrum. Instead of simulating the flux according to

one model, a general uniform flux is used and later reweighted to be able to fit to other models more easily.

- A steep power law indicates very few events at the highest energy bins. This means large CPU time would be necessary to simulate these events. As an example, let us assume two different fluxes

$$f_1 = A \cdot x^{-1}, \quad (\text{D.16})$$

$$f_2 = B \cdot x^{-2}, \quad (\text{D.17})$$

where $A = 10^3$ and $B = 10^4$, so the fluxes cross at a value of $x^{-1+2} = x = \frac{10^4}{10^3} = 10$. In the interval $x \in [10^3, 10^4]$, the number of events for f_1 is equal to 10^3 , whereas for f_2 this is equal to 9.

Simulating with harder spectra* leads to more statistics in high-energy bins.

The weights can be generally written down as

$$w = \frac{dN_{exp}}{dAd\Omega dEdt} \times \frac{dAd\Omega dE}{dN_{sim}}. \quad (\text{D.18})$$

A disadvantage of using weights is that certain events with a high weight are rare but can dominate or obscure the sample in the tails of certain distributions.

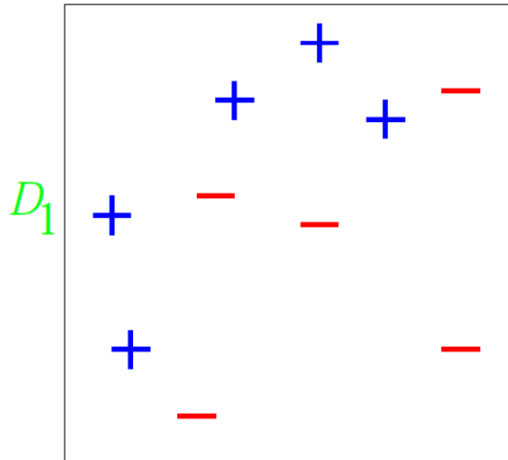
*Harder spectra equals to a lower gamma, since there will be more high-energy events.

E. AdaBoost: simple example

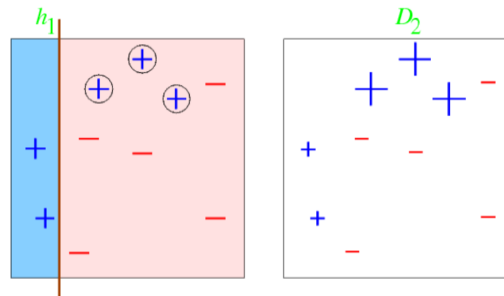
Consider a binary decision tree classification with 10 training examples. The illustrations below are 2D variable distributions.

We give each event an equal weight, making the weight distribution D_1 uniform. For this simple example, each of our classifiers will be an axis-parallel linear classifier (simple cut in one of the two variables).

Initial distribution

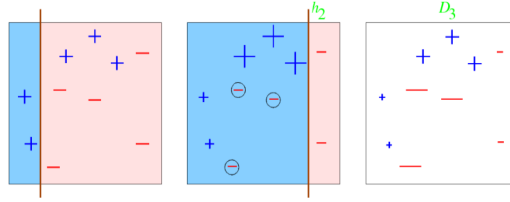


Round 1

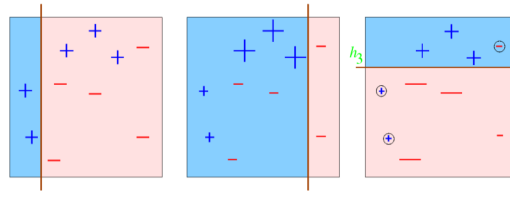


- Error rate of h_1 : $\epsilon_1 = 0.3$; weight of h_1 (see Eq. ??): $\alpha_1 = \frac{1}{2} \ln \left(\frac{1-\epsilon_1}{\epsilon_1} \right) = 0.42$

- An event that is misclassified gets a higher weight: weight multiplied with $\exp(\alpha_1)$
- An event that is correctly classified gets a lower weight: weight multiplied with $\exp(-\alpha_1)$

Round 2

- Error rate of h_1 : $\epsilon_1 = 0.21$; weight of h_2 (see Eq. ??): $\alpha_2 = \frac{1}{2} \ln \left(\frac{1-\epsilon_2}{\epsilon_2} \right) = 0.65$
- An event that is misclassified gets a higher weight: weight multiplied with $\exp(\alpha_2)$
- An event that is correctly classified gets a lower weight: weight multiplied with $\exp(-\alpha_2)$

Round 3

The error rate of h_1 : $\epsilon_1 = 0.21$; weight of h_2 (see Eq. ??): $\alpha_2 = \frac{1}{2} \ln \left(\frac{1-\epsilon_2}{\epsilon_2} \right) = 0.65$
Let us suppose to stop after this round, we now have a forest of 3 decision classifiers: h_1, h_2, h_3 .

Final step

The final classifier is a weighted linear combination of all the classifiers:

$$H_{\text{final}} = \text{sign} \left(0.42 \cdot h_1 + 0.65 \cdot h_2 + 0.92 \cdot h_3 \right)$$

=

3. Some useful things for LaTeX

3.1 Definitions

This is an example of a definition. A definition could be mathematical or it could define a concept.

Definition 3.1.1 — Definition name. Given a vector space E , a norm on E is an application, denoted $\|\cdot\|$, E in $\mathbb{R}^+ = [0, +\infty[$ such that:

$$\|\mathbf{x}\| = 0 \Rightarrow \mathbf{x} = \mathbf{0} \quad (3.1)$$

$$\|\lambda\mathbf{x}\| = |\lambda| \cdot \|\mathbf{x}\| \quad (3.2)$$

$$\|\mathbf{x} + \mathbf{y}\| \leq \|\mathbf{x}\| + \|\mathbf{y}\| \quad (3.3)$$

3.2 Remarks

This is an example of a remark.



The concepts presented here are now in conventional employment in mathematics. Vector spaces are taken over the field $\mathbb{K} = \mathbb{R}$, however, established properties are easily extended to $\mathbb{K} = \mathbb{C}$.

3.3 Corollaries

This is an example of a corollary.

Corollary 3.3.1 — Corollary name. The concepts presented here are now in conventional employment in mathematics. Vector spaces are taken over the field $\mathbb{K} = \mathbb{R}$, however, established properties are easily extended to $\mathbb{K} = \mathbb{C}$.

3.4 Propositions

This is an example of propositions.

3.4.1 Several equations

Proposition 3.4.1 — Proposition name. It has the properties:

$$|||\mathbf{x}|| - ||\mathbf{y}||| \leq ||\mathbf{x} - \mathbf{y}|| \quad (3.4)$$

$$|| \sum_{i=1}^n \mathbf{x}_i || \leq \sum_{i=1}^n ||\mathbf{x}_i|| \quad \text{where } n \text{ is a finite integer} \quad (3.5)$$

3.4.2 Single Line

Proposition 3.4.2 Let $f, g \in L^2(G)$; if $\forall \varphi \in \mathcal{D}(G)$, $(f, \varphi)_0 = (g, \varphi)_0$ then $f = g$.

3.5 Examples

This is an example of examples.

3.5.1 Equation and Text

■ **Example 3.1** Let $G = \{x \in \mathbb{R}^2 : |x| < 3\}$ and denoted by: $x^0 = (1, 1)$; consider the function:

$$f(x) = \begin{cases} e^{|x|} & \text{si } |x - x^0| \leq 1/2 \\ 0 & \text{si } |x - x^0| > 1/2 \end{cases} \quad (3.6)$$

The function f has bounded support, we can take $A = \{x \in \mathbb{R}^2 : |x - x^0| \leq 1/2 + \epsilon\}$ for all $\epsilon \in]0; 5/2 - \sqrt{2}[$. ■

3.5.2 Paragraph of Text

■ **Example 3.2 — Example name.** Nam dui ligula, fringilla a, euismod sodales, sollicitudin vel, wisi. Morbi auctor lorem non justo. Nam lacus libero, pretium at, lobortis vitae, ultricies et, tellus. Donec aliquet, tortor sed accumsan bibendum, erat ligula aliquet magna, vitae ornare odio metus a mi. Morbi ac orci et nisl hendrerit mollis. Suspendisse ut massa. Cras nec ante. Pellentesque a nulla. Cum sociis natoque penatibus et magnis dis parturient montes, nascetur ridiculus mus. Aliquam tincidunt urna. Nulla ullamcorper vestibulum turpis. Pellentesque cursus luctus mauris. ■

3.6 Exercises

This is an example of an exercise.

Exercise 3.1 This is a good place to ask a question to test learning progress or further cement ideas into students' minds. ■

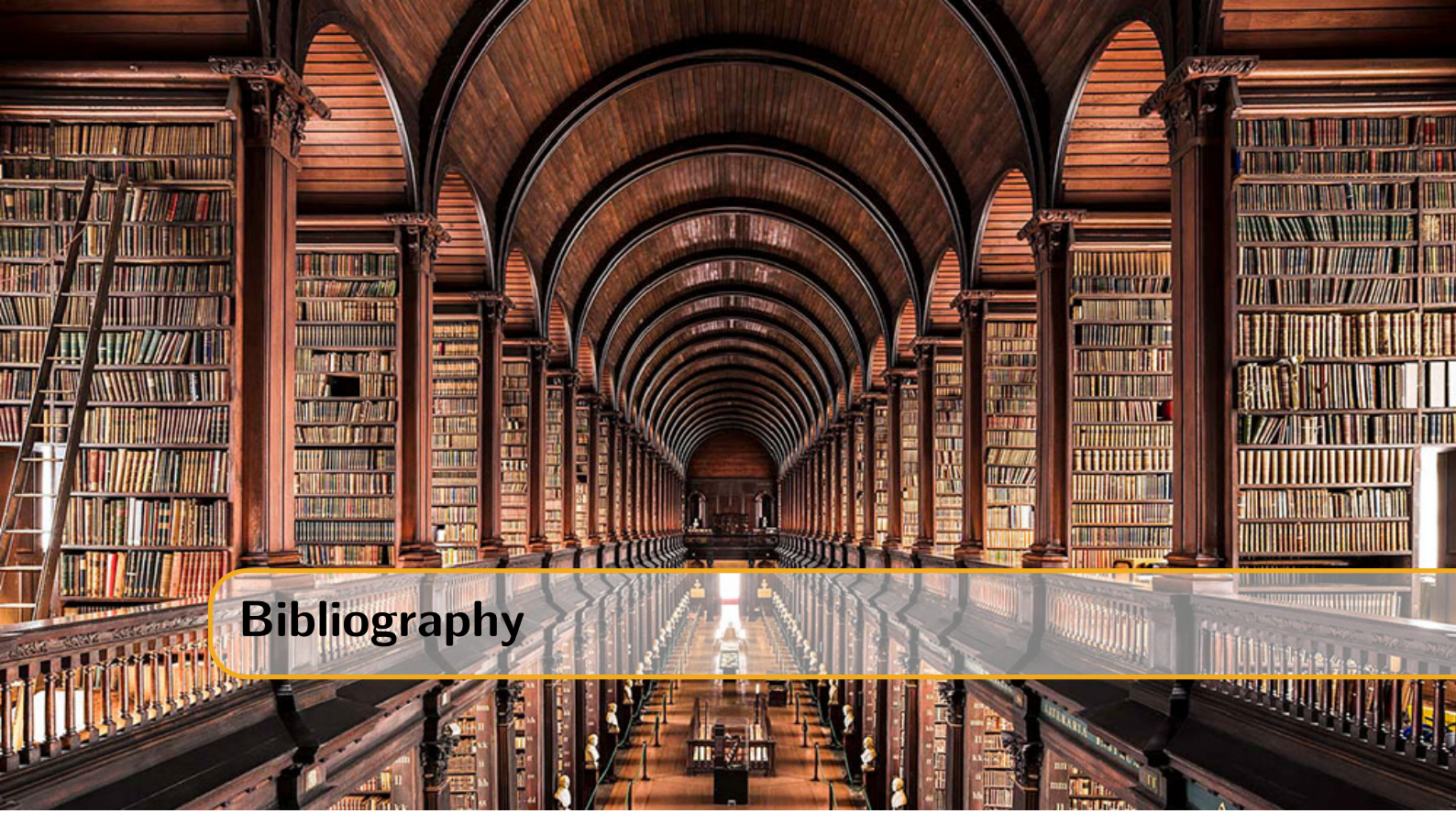
3.7 Problems

Problem 3.1 What is the average airspeed velocity of an unladen swallow?

3.8 Vocabulary

Define a word to improve a students' vocabulary.

Vocabulary 3.1 — Word. Definition of word.



Bibliography

- [1] IceCube collaboration. URL: <https://docushare.icecube.wisc.edu/dsweb/Get/Document-56551/VEFproposal.pdf> (cited on page 7).
- [2] IceCube collaboration. URL: https://docushare.icecube.wisc.edu/dsweb/Get/Document-59303/lowup_2012_proposal.pdf (cited on page 9).
- [3] IceCube collaboration. URL: <https://docushare.icecube.wisc.edu/dsweb/Get/Document-59728/onlinel2proposal2012.pdf> (cited on page 9).
- [4] IceCube collaboration. URL: <https://docushare.icecube.wisc.edu/dsweb/Get/Document-59397/DeepCoreFilterProposal.pdf> (cited on page 9).
- [5] IceCube collaboration. URL: https://wiki.icecube.wisc.edu/index.php/Effects_of_DOM_Mainboard_Release_443 (cited on page 11).
- [6] S. Verpoest. “Search for particles with fractional charges in IceCube based on anomalous energy loss”. Master’s thesis. UGent, 2018 (cited on page 13).



Index

C

Corollaries 37

D

Definitions 37

E

Examples 38

 Equation and Text 38

 Paragraph of Text 38

Exercises 38

P

Problems 38

Propositions 37

 Several Equations 38

 Single Line 38

R

Remarks 37

V

Vocabulary 38